

Ultrafast Photoinduced Melting of a Spin-Peierls Phase in an Organic Charge-Transfer Compound, K-Tetracyanoquinodimethane

H. Okamoto, K. Ikegami, T. Wakabayashi, Y. Ishige, J. Togo, H. Kishida, and H. Matsuzaki

Department of Advanced Materials Science, University of Tokyo, Chiba 277-8561, Japan

(Received 6 July 2005; published 26 January 2006)

Ultrafast photoinduced phase transition in a spin-Peierls (SP) system of K-tetracyanoquinodimethane (K-TCNQ) was studied by femtosecond (fs) reflection spectroscopy. Photocarriers destabilize the SP phase, resulting in a decrease in molecular dimerization within 400 fs. Such a melting of the SP phase drives three kinds of coherent oscillations. By comparing the oscillations with the Raman bands activated by the dimerization, we show that the oscillation of 20 cm^{-1} is due to an LO phonon, and it plays an important role for the stabilization of the SP phase.

DOI: [10.1103/PhysRevLett.96.037405](https://doi.org/10.1103/PhysRevLett.96.037405)

PACS numbers: 78.47.+p, 71.30.+h, 78.30.Jw

Recent developments in fs laser technology have opened up new possibilities for ultrafast control of electronic and crystal structures of solids by irradiation of fs laser pulses. This phenomenon is called photoinduced phase transition (PIPT). PIPTs are now emerging subjects of great interest that need to be investigated extensively since they are important not only as new phenomena in solid-state physics and optical science, but also as useful mechanisms applicable to ultrafast switching operations. Considering applications of PIPTs in switching devices, it is important to control material phases in an ultrafast time scale.

A key strategy toward realizing PIPTs is the exploration of one-dimensional (1D) materials, which include strong instabilities inherent in electron-lattice (e - l) and/or spin-lattice (s - l) interactions and sometimes produce characteristic phase transitions, such as Peierls and spin-Peierls (SP) transitions. In an SP phase, photocarriers are able to stimulate the instability of the s - l system [1], and ultrafast melting of the SP phase is expected. In fact, photoinduced destabilization of the SP phase was suggested to occur in an organic charge-transfer (CT) compound, K-tetracyanoquinodimethane (K-TCNQ) [2], and a neutral radical crystal, trithiatriazapentalenyl [1]. However, their fs dynamics have not yet been investigated.

In the present study, we focus on K-TCNQ, which is composed of TCNQ chains as illustrated in Fig. 1a-[i] [3]. An electron is transferred from K to TCNQ and a TCNQ⁻ chain forms a half-filled π -electron band. From the theoretical point of view, a 1D half-filled system has a finite gap for any nonzero on-site Coulomb repulsion, U , and then becomes a Mott insulator [4]. In K-TCNQ, U is much larger than the electron transfer energy, t , between adjacent molecules [5,6]. This type of Mott insulators can be considered to be an antiferromagnetic spin ($S = 1/2$) chain, which is sometimes converted to a dimerized diamagnetic state at low temperatures [7]. This transition, called an SP transition, is caused by the magnetic-energy gain due to the spin-singlet formation overcoming the lattice distortion energy. The key factor in the SP transition is the s - l interaction determining the magnitude of the modulation

of the antiferromagnetic exchange coupling, J , between adjacent two spins by dimeric molecular displacements [7]. K-TCNQ shows a phase transition at $T_c = 395\text{ K}$ [8], below which TCNQ molecules are dimerized (Fig. 1a-[ii]). The temperature dependence of the x-ray reflection intensity activated by the dimerization is plotted by open circles in Fig. 1, showing that the dimeric displacements gradually increase with decreasing temperature below T_c [8]. As shown in Fig. 1(b), the spin susceptibility χ_p sharply decreases below T_c [9]. χ_p in the high-temperature (T) phase could be explained by assuming a uniform antiferromagnetic spin ($S = 1/2$) chain, indicating the SP nature of this transition [10]. Other theoretical studies also suggested that this transition is driven by the SP mechanism [11,12].

In this Letter, we report the ultrafast dynamics of the photoinduced melting of the SP phase in K-TCNQ investigated by fs pump-probe (PP) reflection spectroscopy. Irradiation of a fs laser pulse produces localized electron

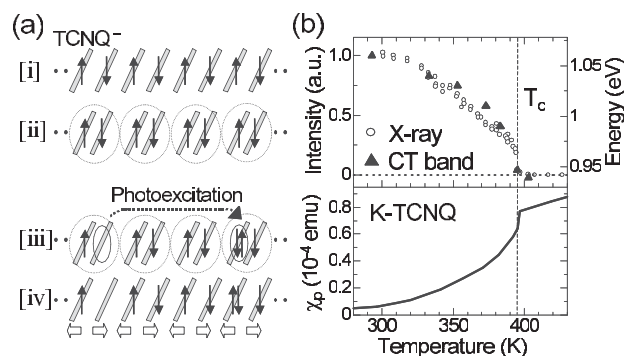


FIG. 1. (a) Schematic views of [i] the regular TCNQ⁻ chain, [ii] the dimerized SP phase, [iii] the photoexcitation of an electron-hole pair, and [iv] the dissolution of the dimerization. (b) Upper panel: temperature dependence of the x-ray reflection intensity (open circles) reflecting the dimerization (taken from Ref. [8]) and the peak energy of the CT band (solid triangles). Lower panel: temperature dependence of the spin susceptibility (taken from Ref. [9]).

and hole carriers, which form nonmagnetic sites and then destabilize the SP phase. That results in the melting of the SP phase within ~ 400 fs, which is accompanied by three kinds of coherent oscillations with frequencies of 20, 49, and 90 cm^{-1} . By comparing these oscillations with the Raman bands activated by the dimerization, we demonstrate that the 20 cm^{-1} oscillation is assigned to the LO phonon mode in the ground state and this mode plays a significant role in the stabilization of the SP phase.

Single crystals of K-TCNQ were grown from KI and TCNQ through slow diffusion in acetonitrile. For the fs PP reflection spectroscopy, a Ti:Al₂O₃ regenerative amplifier was employed as the light source. The output from the amplifier (800 nm, 1 kHz) with a pulse width of 110 fs was divided into two beams. One beam was used for the pump pulse, and the other for the excitation of an optical parametric amplifier, from which the probe pulses (0.1 to 2.5 eV) were obtained. The time resolution of the apparatus is ~ 150 fs. Polarized Raman spectra were measured using a Raman spectrometer equipped with a He-Ne laser (1.96 eV) and an optical microscope.

Figure 2(a) shows the polarized reflectivity (R) spectrum at 293 K for the light polarization \mathbf{E} parallel to the TCNQ stacking axis \mathbf{a} ($\mathbf{E} \parallel \mathbf{a}$), which is composed of a broad peak around 1 eV and sharp structures due to the intramolecular vibrational modes below 0.3 eV. The broad peak is due to the CT transition, $(\text{TCNQ}^-, \text{TCNQ}^-) \rightarrow (\text{TCNQ}^0, \text{TCNQ}^{2-})$ [5,6]. The open circles show the excitation profile of the photoconductivity (PC) along \mathbf{a} at 77 K ($\mathbf{E} \parallel \mathbf{a}$). The details of the PC measurements were reported elsewhere [13]. The photocurrent is negligible at the CT transition peak indicating that the lowest excited state is a CT exciton. With an increase in energy, the PC gradually increases and then is saturated at ~ 1.5 eV, above which unbound electrons and holes are photogenerated. In Fig. 2(b), photoinduced reflectivity changes, ΔR , spectra with a pump pulse of 1.55 eV (the electric field $\mathbf{E}_{\text{ex}} \parallel \mathbf{a}$) are presented for several delay times t_d . The photon density of a pump pulse absorbed within the absorption depth is ~ 0.095 photon/TCNQ, which is evaluated from the absorption coefficient and the reflection loss for the pump light. At $t_d = 0$ ps, the reflectivity decreased over a wide energy region (0.5–1.8 eV), which is due to the bleaching of the CT band. In the region below 0.5 eV, the reflectivity increased, showing a midgap absorption at ~ 0.25 eV. The PC results suggest that the 1.55 eV excitation generates an unbound electron-hole pair (Fig. 1a-[iii]). The midgap absorption can therefore be attributed to localized carriers or equivalently small polarons stabilized via the e - I interaction. Figure 3(a) shows the time profile of $\Delta R/R$ at 0.25 eV, which is not a simple exponential curve. If we define the decay time τ_{pc} of the photocarriers as the time at which the signal is equal to $1/e$ of the maximum of $\Delta R/R$, τ_{pc} is evaluated to be ~ 3 ps.

In the region of the CT band, the ΔR spectrum shows a characteristic time dependence. Just after the photoirradiation,

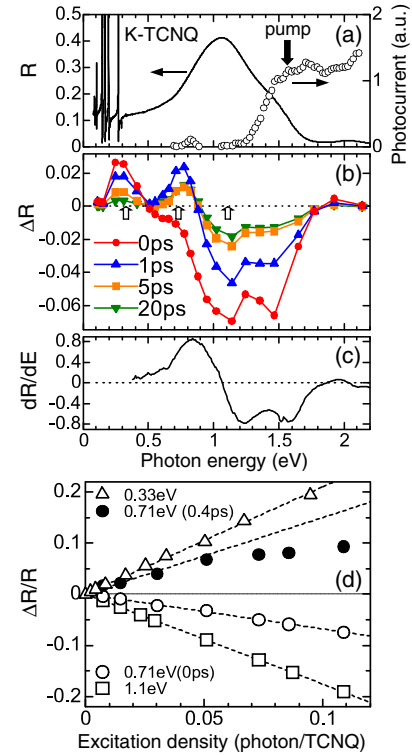


FIG. 2 (color online). (a) Polarized reflectivity (R) spectrum and the excitation profile of the photocurrent along \mathbf{a} (open circles). (b) Photoinduced reflectivity changes (ΔR) spectra. The pump energy is 1.55 eV [the solid arrow in (a)] and the excitation density is 0.095 photon/TCNQ. Open arrows show the energy positions, at which the excitation-density dependences of $\Delta R/R$ are presented in (d). (c) dR/dE spectrum. (d) Excitation-density dependence of $\Delta R/R$.

tion, ΔR is negative for the entire CT-band region (0.5–1.8 eV). At $t_d = 1$ ps, however, ΔR becomes positive in the lower energy region at 0.5–0.9 eV. The spectral shape of ΔR ($t_d = 1$ ps) is very similar to the first derivative of the original reflectivity dR/dE shown in Fig. 2(c). This suggests that photocarriers induce a redshift of the CT band within 1 ps. In K-TCNQ, the peak energy of the CT band, E_{CT} , is correlated with the degree of dimerization. As shown in Fig. 1(b), E_{CT} gradually decreases with temperature. This temperature dependence is in good agreement with that of the dimerization [open circles in Fig. 1(b)] [8]. Such a correlation suggests that the transient redshift of the CT band is due to the photoinduced decrease of the dimerization. Thus, the observed phenomena can be explained as follows. Photogenerated electron and hole carriers are immediately relaxed to small polarons. These polarons form nonmagnetic sites (solid ovals in Fig. 1a-[iii]), which induce not only the breaking of the spin singlets in dimers, but also the destabilization of the SP phase, since the SP state is characteristic of an infinite spin chain. Then they give rise to the dissolution of the dimeric molecular displacements over a long range along the chain (Fig. 1a-[iv]). This results in the redshift of the CT band.

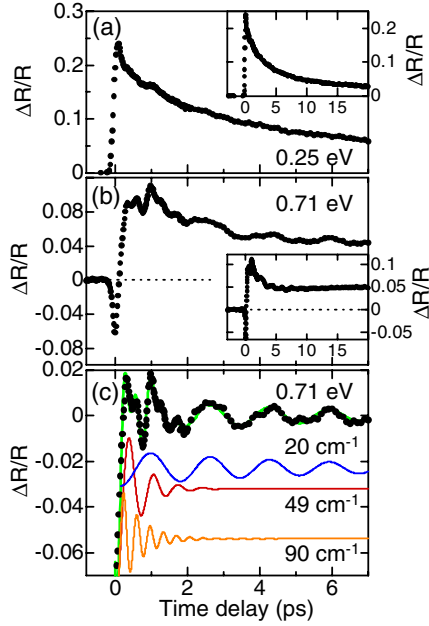


FIG. 3 (color online). (a),(b) Time profiles of $\Delta R/R$ at (a) 0.25 eV and (b) 0.71 eV. (c) Oscillatory components (solid circles) extracted from (b). The thin solid line is a fitting curve, which is the sum of the three damped oscillators shown in the lower region.

Such a photoinduced phenomenon is analogous to the impurity effect of the SP system, CuGeO_3 , in which the SP transition is suppressed by the introductions of non-magnetic impurities [14]. The theoretical studies also demonstrated that the magnetic-energy gain due to the SP dimerization is decreased in finite spin chains [15].

We can now discuss the dynamical aspects of the PIPT. ΔR at ~ 0.7 eV characterizes the redshift of the CT band and reflects directly the dynamics of the photoinduced melting of the SP phase. The time profile of $\Delta R/R$ at 0.71 eV is shown in Fig. 3(b). First, the reflectivity decreases due to the bleaching of the CT band. In this process, the SP dimerizations are not changed. Subsequently, the reflectivity increases up to $t_d \sim 400$ fs due to the redshift of the CT band caused by the decrease of the dimeric displacements. Its time scale will be determined by lattice phonons associated with the dimerization (the SP modes). Since the midgap absorption appears within the time resolution [Fig. 3(a)], the localization of photocarriers, that is, the small-polaron formation, should be attributed to the higher-frequency phonons different from the SP modes. It suggests that the e - l and s - l interactions are dominated by different phonon modes. After the delayed increase of $\Delta R/R$, prominent oscillations are observed. These oscillations are attributable to the changes of the equilibrium molecular positions induced by the dissolution of the dimeric displacements.

To analyze the oscillations, we extracted the oscillatory component by subtracting the background rise and decay from $\Delta R/R$, which is plotted in Fig. 3(c). This oscillatory

component can be reproduced well by using the sum of the three cosine-type damped oscillators expressed by the following formula, as shown by the thin-solid line:

$$\frac{\Delta R}{R} = \sum_i A_i \cos(\omega_i t - \phi_i) \times \exp(-t/\tau_i); (i = 1, 2, 3), \quad (A_i < 0). \quad (1)$$

The three components are also shown in the figure. The frequencies ω_i (the decay times τ_i) of the three modes are 20 cm^{-1} (5.7 ps), 49 cm^{-1} (0.53 ps), and 90 cm^{-1} (0.57 ps). The initial phase ϕ_i is almost equal to zero. The 20 cm^{-1} oscillation is relatively long-lived.

The phonon modes corresponding to the dimerization are Raman active only in the SP phase and show specific selection rules for light polarization depending on the directions of the displacements. Therefore, polarization dependence of the Raman spectra should be useful for the clarification of the origins of the coherent oscillations. Raman spectra at $293 \text{ K} (< T_c)$ and $400 \text{ K} (> T_c)$ are presented in Fig. 4(a), where x corresponds to the chain axis \mathbf{a} and z indicates the direction of the incident light. The bands A–E are attributable to the zone-boundary modes in the high- T phase, which are activated in the SP phase by the zone folding [16]. These bands will include the modes related to the dimerization. The frequency (20 cm^{-1}) of the long-lived oscillation is equal to that of band A, so that it is attributed to the lattice mode of the dimerized SP ground state. When the dimeric displacements average out to zero after the photoirradiation, the coherent oscillation corresponds with the zone-boundary mode in the high- T phase. In this case, the frequency of the oscillatory

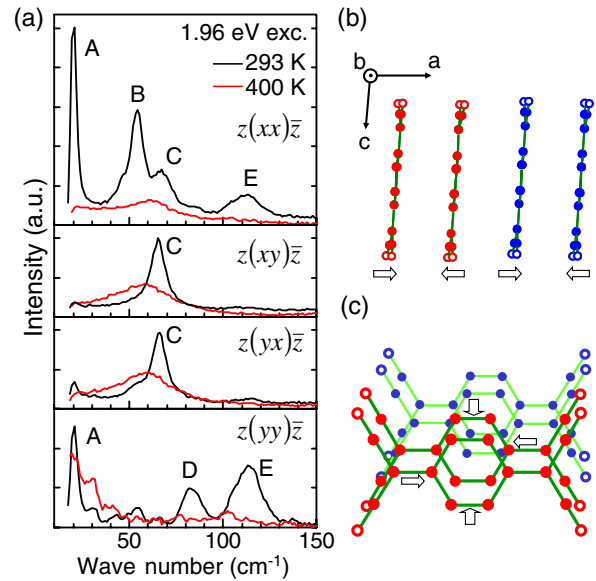


FIG. 4 (color online). (a) Polarized Raman spectra for the incident light of 1.96 eV at 293 K and at 400 K. x corresponds to the chain axis \mathbf{a} and z shows the direction of the incident light. (b),(c) Structures viewed (b) along \mathbf{b} and (c) along \mathbf{a} [5]. The arrows indicate molecular displacements.

signal in $\Delta R/R$ will be doubled. If anharmonicity causes the coherence of the oscillation to be lost, the oscillatory signal may disappear. The observation of the coherent oscillation with the same frequency as the Raman mode (20 cm^{-1}) indicates that the dimerization was not completely lost by the photoirradiation in our case. Band A is strongly activated for $z(xx)\bar{z}$, so that it can be assigned to the LO mode corresponding to the dimerization along \mathbf{a} as illustrated in Fig. 4(b). The decay time (5.7 ps) of the 20 cm^{-1} oscillation is much longer than that of photocarriers $\tau_{\text{pc}} \sim 3$ ps. Namely, this oscillation survives without disturbance of the coherence even after the photocarriers decay. It demonstrates that this oscillation is due to the phonon mode of the SP ground state. Coherent oscillations related to the instabilities of the $e-l(s-l)$ systems induced by photoirradiations have also been reported in the insulating phase of VO_2 [17], the neutral and ionic phases of TTF-CA (TTF = tetrathiafulvalene and CA = chloranil) [18], and the charge-order phase in $(\text{EDO-TTF})_2\text{PF}_6$ (EDO-TTF = ethylenedioxytetrathiafulvalene) [19].

For the oscillations of 49 and 90 cm^{-1} , no Raman bands are observed at the same frequencies. In addition, the decay time (~ 0.5 ps) is much shorter than τ_{pc} . Therefore, these oscillations are attributable to the local phonon modes in the photoexcited states. Possible assignments are transverse modes. In K-TCNQ, dimeric displacements exist along the two molecular axes as well as along \mathbf{a} , as indicated by the arrows in Fig. 4(c), wherein molecular overlaps along the direction normal to the molecular planes at 298 K are illustrated [3]. Since the normal to the molecular planes is inclined $\sim 16^\circ$ to \mathbf{a} , the transverse displacement, that is, the TO mode, can cause the dimerization. The important point is that the coherent oscillation selectively excited in the ground state should be the phonon mode driving the SP transition, which is the LO mode in K-TCNQ, whereas the TO modes will not play significant roles for the stabilization of the SP phase. Such information about a transition mechanism cannot be obtained from the usual x-ray studies.

The positive $\Delta R/R$ signal at 0.71 eV showing the melting of the SP phase decreases up to 5 ps and then becomes almost constant up to 20 ps [the inset of Fig. 3(b)]. The initial decrease is attributable to the recovery of the dimerization following the decay of photocarriers with $\tau_{\text{pc}} \sim 3$ ps. The decay of photocarriers leads to the increase of the temperature of the $s-l$ system, which is the origin for the residual $\Delta R/R$ component, since the increase of temperature induces a decrease of E_{CT} [Fig. 1(b)]. This long-lived component decays with a time scale of microseconds [2]. Except for such thermal effects, the photoinduced melting of the SP phase and its recovery occur very fast within ~ 400 fs and ~ 5 ps, respectively.

Finally, we briefly discuss the excitation-density (I_{ph}) dependence of the photoinduced melting of the SP phase. I_{ph} dependence of $\Delta R/R$ is presented in Fig. 2(d).

$|\Delta R/R(t_d = 0\text{ ps})|$ is proportional to I_{ph} up to 0.1 photon/TCNQ for three typical probe energies indicated by the open arrows in Fig. 2(b). The solid circles show the I_{ph} dependence of $\Delta R/R(t_d = 0.4\text{ ps})$ at 0.71 eV, which indicates the efficiency of the melting of the SP dimerizations. $\Delta R/R(t_d = 0.4\text{ ps})$ at 0.71 eV is saturated for $I_{\text{ph}} > 0.05$ photon/TCNQ, being in contrast to the linear I_{ph} dependence of $|\Delta R/R(t_d = 0\text{ ps})|$ at the same energy. A possible reason for this saturation is the space filling of weakly dimerized domains induced by photoirradiation. If the space filling is assumed to be completed for $I_{\text{ph}} = 0.05$ photon/TCNQ, the domain size converted by one photon is estimated to be ~ 20 TCNQ molecules. By comparing $\Delta R/R(t_d = 0.4\text{ ps}) - \Delta R/R(t_d = 0\text{ ps})$ with dR/dE at 0.71 eV, we found ΔE_{CT} to be 0.04 eV for $I_{\text{ph}} = 0.05$ photons/TCNQ, which is $\sim 40\%$ of the shift of the CT band (0.11 eV) between the SP phase at 293 K and the undimerized phase at 396 K. This value ($\sim 40\%$) gives a rough estimation of the decrease of the dimeric displacement for $I_{\text{ph}} = 0.05$ photon/TCNQ. To obtain more precise information about the photoinduced changes in dimeric displacements, time-resolved x-ray studies should be necessary.

In summary, photoirradiation of K-TCNQ using a fs laser pulse induces the decrease of the dimerizations within ~ 400 fs through the destabilization of the SP phase due to the photocarrier generations. Such a melting of the SP phase drives the coherent oscillation with 20 cm^{-1} due to the LO mode which plays an important role in the stabilization of the SP phase.

-
- [1] H. Matsuzaki *et al.*, Phys. Rev. Lett. **91**, 017403 (2003).
 - [2] S. Koshihara *et al.*, Phys. Rev. B **44**, 431 (1991).
 - [3] M. Konno *et al.*, Acta Crystallogr. B **33**, 763 (1977).
 - [4] E. H. Lieb and F. Y. Wu, Phys. Rev. Lett. **20**, 1445 (1968).
 - [5] K. Yakushi *et al.*, Chem. Phys. Lett. **68**, 139 (1979).
 - [6] H. Okamoto *et al.*, Phys. Rev. B **36**, 3858 (1987).
 - [7] J. W. Bray, L. V. Interrante, I. S. Jacobs, and J. S. Miller, in *Extended Linear Chain Compounds*, edited by J. S. Miller (Plenum Press, New York, 1983), Vol. 3, p. 353.
 - [8] H. Terauchi, Phys. Rev. B **17**, 2446 (1978).
 - [9] J. G. Vegter and J. Kommandeur, Chem. Phys. Lett. **3**, 427 (1969).
 - [10] Y. Lepine *et al.*, Phys. Rev. B **18**, 3585 (1978).
 - [11] Y. Takaoka and K. Motizuki, J. Phys. Soc. Jpn. **47**, 1752 (1979).
 - [12] Y. Lepine, Phys. Rev. B **28**, 2659 (1983).
 - [13] M. Ono *et al.*, Phys. Rev. B **70**, 085101 (2004).
 - [14] M. Hase *et al.*, Phys. Rev. Lett. **71**, 4059 (1993).
 - [15] D. Guo *et al.*, Phys. Rev. B **41**, 9592 (1990).
 - [16] M. Yoshikawa *et al.*, J. Phys. Soc. Jpn. **55**, 1177 (1986).
 - [17] A. Cavalleri *et al.*, Phys. Rev. B **70**, 161102 (2004).
 - [18] H. Okamoto *et al.*, Phys. Rev. B **70**, 165202 (2004).
 - [19] M. Chollet *et al.*, Science **307**, 86 (2005).